Ag on Ge(111): 2D X-ray structure analysis of the $\sqrt{3} \times \sqrt{3}$ superstructure

D. Dornisch, W. Moritz, H. Schulz

Institute of Crystallography and Mineralogy, University of Munich, Theresienstrasse 41, D-8000 München 2, Germany

R. Feidenhans'l, M. Nielsen, F. Grey

Risø National Laboratory, DK-4000 Roskilde, Denmark

R.L. Johnson

II. Institute for Experimental Physics, University of Hamburg, D-2000 Hamburg 50, Germany

and

G. Le Lay

CRMC 2-CNRS, Campus de Luminy, Case 913, 13288-Marseille Cedex 09, France

We have studied the Ag/Ge(111)$\sqrt{3} \times \sqrt{3}$ superstructure by grazing-incidence X-ray diffraction. In our structural analysis we find striking similarities to the geometry of Au on Si(111). The Ag atoms form trimer clusters with an Ag–Ag distance of 2.94 ± 0.04 Å with the centers of the trimers being located at the origins of the $\sqrt{3} \times \sqrt{3}$ lattice. The Ag layer is incomplete and at least one substrate layer is distorted.

1. Introduction

Structures of thin layers of noble metals on elemental semiconductor surfaces have been the subject of a large number of studies with various methods in the last ten years. A survey of older literature is given by Le Lay [1]. Surprisingly little work has been performed on the system Ag/Ge(111). Like Ag and Au on Si(111) it forms a $(\sqrt{3} \times \sqrt{3})$R30° structure at a coverage of about 1 monolayer (ML) [1]. To our knowledge there exists no structural model for this surface.

Photoelectron spectroscopy with Ag on Ge(111) shows noticeable similarities with the electronic structure of Ag on Si(111) [3–4], which makes structural similarities between both systems very likely. Fan and Ignatiev [5] observed LEED *IV* curves for the $\sqrt{3} \times \sqrt{3}$ structures of Ag/Ge(111), Ag/Si(111) and for the metastable $\sqrt{3} \times \sqrt{3}$ reconstructions of the clean Ge(111) and Si(111) surfaces, which were very alike. From this, they drew the conclusion, that in both adsorbate systems the $\sqrt{3} \times \sqrt{3}$ structure is not caused by a well-ordered layer of adatoms, but results from a reconstruction of the topmost substrate layers, which would be stabilized by the adatoms.

Strong resemblance between Au/Si(111) and Ag/Ge(111) has been observed as well. In a careful AES study, Bertucci et al. [6] found a saturation coverage of $\theta_{Ag} = 0.85 \pm 0.05$ ML for the completion of a 2D Ag adlayer with $\sqrt{3} \times \sqrt{3}$ structure. This value is practically identical with

the saturation coverage of the $\sqrt{3} \times \sqrt{3}$ structure of Au on Si(111) as determined recently with medium-energy ion scattering (MEIS) by Chester et al., i.e. 0.84 ± 0.05 ML [7]. It is further remarkable that Ag deposition on a $\sqrt{3} \times \sqrt{3}$ reconstructed Ag/Ge(111) surface leads to a 2D phase with 6×6 reconstruction. A 6×6 reconstruction is not observed in the Ag/Si(111) system but in Au/Si(111).

It should be noted that Suliga and Henzler [8] observed with LEED a facetting of the Ge(111) surface after Ag adsorption at substrate temperatures above 350°C, which is associated with large mass transport along the surface. The facetting may explain some of the experimental difficulties in obtaining reproducible data.

In this work, we present the results of a X-ray structural analysis of the $\sqrt{3} \times \sqrt{3}$ superstructure of Ag on Ge(111) and find striking similarities to the previously studied $\sqrt{3} \times \sqrt{3}$ structure of Au on Si(111) [9].

2. Experimental

The measurements were performed at the synchrotron laboratory HASYLAB at DESY in Hamburg. The sample preparation was performed at the photoemission beamline FLIPPER II. The Ge(111) surfaces were cleaned by 500 eV Ar^+-ion bombardement and subsequent anneal to 720°C. This procedure was repeated until a sharp c(2 × 8) LEED pattern emerged and the angle-integrated photoemission showed no traces of impurities. Ag was evaporated from a Knudsen cell held at 840°C at a rate of 1.5 Å/min. About 20 Å Ag was deposited on the surface. The sample was then transferred to a portable X-ray ultrahigh-vacuum cell which was mounted on the vertical scattering diffractometer at the X-ray wiggler beamline W1.

The white X-ray beam was monochromatized by two Si(111) crystals to a wavelength of 1.305 Å. A 1 mm slit (in the surface plane) was placed just before the sample and a 1.5 mm slit was placed on the detector arm behind the sample. These slits defined the active area of the Ge(111) surface in the experiment. The detector was a position-sensitive gas-filled wire counter (Braun

OED-50) suspending 0.6° in the surface plane and 2.7° out of the plane.

As deposited, the Ag forms a homogeneous, quasi-epitaxial film with (111)Ag∥(111)Ge and (110)Ag∥(110)Ge. Small amounts of Ag were rotated 30° in the surface plane away from these directions. Only a very weak signal from a $\sqrt{3} \times \sqrt{3}$ layer could be detected.

Heating the sample to about 150°C, the Ag film coalesced into 3D clusters connected by a 2D layer. This was very clear from the behavior of the intensities along the Bragg rods in the direction normal to the surface. A sharp and strong signal from a $\sqrt{3} \times \sqrt{3}$ layer was observed. The intensities of the fractional-order Bragg rods were in the order of magnitude as expected from a monolayer of silver atoms. The width of the peaks in the omega scans corresponded to a coherence length of 400–500 Å. We used this surface to collect a set of structure factors of the $\sqrt{3} \times \sqrt{3}$ structure to be used in the crystallographic determination.

The samples were aligned such that a fixed angle of incidence of 0.6° was kept throughout the data collection. Integrated intensities were measured by collecting the total (background-corrected) intensity in omega scans around the surface normal for a set of fractional-order in-plane reflections. Symmetry-equivalent reflections were averaged and corrected for Lorentz factors and variation in active area to obtain a set of structure factor amplitudes for non-equivalent reflections. The uncertainties were estimated on the basis of reproducibility between the intensities of symmetry-equivalent reflections. Two samples were measured. The data were within uncertainty identical, however, due to its better quality, only one set was analyzed further.

The structural analysis is based on a set of 17 symmetry-inequivalent fractional-order reflections. The reflections are labelled with respect to the $\sqrt{3} \times \sqrt{3}$ superstructure cell. One of the reflections, the (1,2) reflection, has an intensity that is more than one order of magnitude stronger than all the others. This requires a carefull discussion of the applied weighting scheme to ascertain that the refinement would not be dominated by only one reflection.

3. Results

Direct information about the atomic geometries can be obtained by a contour plot of the Patterson (or autocorrelation) function $P(x,y)$:

$$P(x,y) = \sum_{hk} |F_{hk}|^2 \cos(hx + ky).$$

This gives a map of the interatomic vectors inside the unit cell. The height of a peak in the map scales as $Z_1 \cdot Z_2$, Z_1 and Z_2 being the atomic numbers of the two atoms involved. The use of the superstructure reflections only leads to a partial Patterson function showing the difference of the superstructure to an averaged 1×1 structure. The positive peaks can be identified with interatomic vectors in the adsorbate layer in simple adsorbate structures. Because integer-order reflections are excluded from the analysis the registry between the superstructure and the underlying bulk lattice cannot be determined. The integer-order reflections were left out because of possible inhomogenities of the surface. However,

the fractional-order reflections contain the complete information about the reconstructed atoms. Fourier synthesis with this subset of reflections gives the difference structure between the superstructure and an averaged structure, which would be the result of superpositioning all 1×1 subcells of the $\sqrt{3} \times \sqrt{3}$ unit cell [10].

The Patterson functions of the $\sqrt{3} \times \sqrt{3}$ superstructures of Au/Si(111) and Ag/Ge(111) shown in fig. 1 are remarkably similar. In both cases only one peak occurs in the irreducible unit with an interatomic distance between 2.6 and 2.9 Å. This suggests that the Ag atoms form trimer clusters located on top of the substrate as Au does on Si(111) [9]. In addition distortions of substrate layers become visible in the shape of the Patterson peak. The stronger broadening of the Patterson peak of Ag/Ge(111) is a consequence of the smaller difference in atomic number between Ag ($Z = 49$) and Ge ($Z = 32$) than that between Au ($Z = 79$) and Si ($Z = 14$) (table 1). The Patterson function gives direct evidence for the trimer
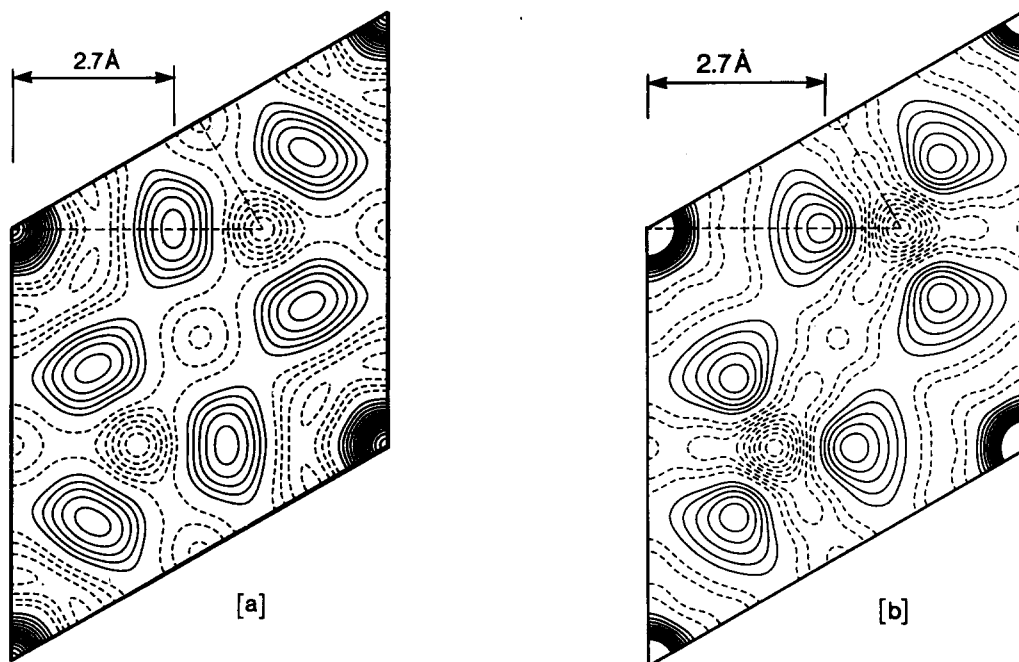

Fig. 1. (a) Patterson function of Ag/Ge(111)$\sqrt{3} \times \sqrt{3}$. (b) Patterson function of Au/Si(111)$\sqrt{3} \times \sqrt{3}$. The irreducible units are marked by dashed lines. The non-trivial maxima are scaled to the same height.

model. Nevertheless, because of the similarity with the system Ag/Si(111) and the different structure found there [11,12] we investigated that structure model as well.

In the calculations for the trimer models we choose as a starting point for the structural analysis a model with only a single Ag layer. Distortions in the substrate should come out when applying a difference Fourier synthesis. Assuming that the phases of the model structure factors are correct, the difference Fourier synthesis is the difference between the real (measured) electron density and the model electron density. A contour map will therefore highlight missing or wrong parts in the model structure [13]. Refinement of this starting model terminates with a very high R value [14] of 57%. The difference–electron-density map shows only one peak located close to ($\frac{2}{3}$,0) representing a split-atom, which we consider is due to a distorted substrate layer. This applies to one half of the double layer. There is no evidence for a distortion of the second half of the double layer. This means that the second half of the double layer is either missing or its atoms are sitting at high symmetric positions and are therefore not visible in the analysis of the superstructure reflections only.

If the split-position is occupied with 0.5 Ge atom after refining all atomic coordinates, individual isotropic Debye–Waller factors and relative occupancies, an R value of 3.1% and a goodness-of-fit (GOF) [14] of 13.6 are obtained, when using unity weighting. Using individual weights based on counting statistics and reproducibility between symmetric equivalent reflections, the R value rises to 36%, but the GOF drops to 4.6. (tables 2 and 3). This is related to the fact that the data set is dominated by one

reflection, namely (1,2), which represents 70% of the total scattered intensity. In the refinement with unit weights, it decreases the R value by increasing the denominator while making no contribution to the sum of deviations in the numerator. Fitting adapts best to the strongest reflection, neglecting the weaker ones; nevertheless, the other calculated intensities correspond very well with the ones observed. The relatively high GOF indicates that the applied weights underestimate the uncertainties in the data, and hence the estimated errors of the refined parameters may be too low. Using the individual weights, the GOF decreases but the R value rises dramatically. To check our argumentation we repeated both calculations without the (1,2) reflection. Then the R value for the individual weighted refinement again gives 36%, and the R value with unity weighting rises to 29%, thus proofing that indeed the (1,2) reflection is responsible for the discrepancy in the R values of the fits with different weighting schemes. However, it must be emphasised that both weighting schemes lead to nearly identical structural parameters in the refinement process including individual weighted refinement without (1,2) reflection. A trimer model for Ag on Ge can be concluded, but discussion of details, such as the temperature factor and the exact Ag coverage, is limited. Table 3 shows the observed and calculated structure factors for the final model from the refinement with unit weights and with individual weights. The electron density map in the first case is depicted in fig. 2a.

Table 2
Structural parameters of final model

Atom	x	y	θ	B
(a) Refining with unit weights				
Ag	0.245(3)	0.000	0.72(5)	6.9(6)
Ge	0.620(2)	0.068(2)	0.5	2.9(4)
(b) Refining with individual weights				
Ag	0.252(7)	0.000	0.71(8)	6.6(17)
Ge	0.618(4)	0.066(4)	0.5	2.0(5)

Refined values are underlined. The coordinates are given with respect to the $\sqrt{3} \times \sqrt{3}$ unit cell shown in fig. 2b. $\theta_{Ge} = 0.5$ is the occupation factor for one split position and corresponds to one complete Ge layer, i.e. half a double layer.

Table 1
Relative weights of the Patterson peaks in the systems Ag/Si and Au/Si

Vector between	$Z1 \times Z2$	Vector between	$Z1 \times Z2$
Ag–Ag	2209	Au–Au	6241
Ag–Ge	1504	Au–Si	1106
Ge–Ge	1024	Si–Si	196

The main features of the structure seem to be identical to the corresponding Au-on-Si structure. The Ag atoms form trimer clusters centered at the origin of the $\sqrt{3} \times \sqrt{3}$ unit cell. The refined Ag–Ag distance of 2.94 ± 0.04 Å agrees well with the bulk value of 2.89 Å. The distortion of the substrate layer with a shift of 0.42 Å of the Ge atoms away from their ideal bulk positions is slightly less than that in the Au–Si system where a shift of 0.50 Å for the Si atoms was found.

The relative coverage of Ag results from the refinement of the occupation factor for Ag, keeping the occupation factor for Ge fixed at 0.5 for the split positions, i.e. a complete substrate layer. The result is that the Ag layer seems to be incomplete and the average coverage amounts to $\theta_{Ag} = (0.72 \pm 0.05)$ ML. This value corresponds within its error limit closely to the saturation coverage of $\theta_{Ag} = 0.85 \pm 0.05$ ML found by Bertucci et al. [6]. However, the data interpreta-

Table 3
Observed and calculated intensities of final model (F_o^2 is scaled to the sum of F_c^2)

H	K	F_o^2	F_c^2	$\sigma(F_o^2)$	$(F_o^2 - F_c^2)/\sigma(F_o^2)$
(a) Refining with unit weights [a]					
0	1	16.4	100.9	8.9	−9.4834
1	2	4977.0	4970.7	642.2	0.0098
2	3	148.0	185.6	21.4	−1.7571
3	4	128.4	105.8	17.8	1.2655
4	5	112.3	27.1	16.1	5.3091
0	2	144.4	184.4	19.6	−2.0365
1	3	387.1	401.1	101.7	−0.1386
2	4	231.9	287.7	142.7	−0.3915
3	5	183.7	141.3	48.2	0.8791
0	4	308.6	295.8	74.9	0.1697
1	5	112.3	130.6	53.5	−0.3422
2	6	17.8	4.5	7.1	1.8557
0	5	153.4	128.6	41.0	0.6033
1	6	55.3	68.7	26.8	−0.5039
2	7	37.4	57.1	17.8	−1.1021
0	7	10.7	14.2	3.6	−0.9918
0	8	7.1	0.8	5.4	1.1803
(b) Refining with individual weights [b]					
0	1	23.7	45.0	12.9	−1.6515
1	2	7205.3	4910.3	929.7	2.4684
2	3	214.3	215.7	31.0	−0.0445
3	4	185.9	191.2	25.8	−0.2039
4	5	162.7	58.6	23.2	4.4774
0	2	209.1	240.0	28.4	−1.0859
1	3	560.4	659.2	147.2	−0.6713
2	4	335.7	357.2	206.6	−0.1041
3	5	266.0	234.7	69.7	0.4486
0	4	446.7	308.8	108.5	1.2718
1	5	162.7	188.6	77.5	−0.3351
2	6	25.8	12.6	10.3	1.2749
0	5	222.1	120.5	59.4	1.7102
1	6	80.0	104.8	38.7	−0.6390
2	7	54.2	127.2	25.8	−2.8263
0	7	15.4	12.2	5.2	0.6238
0	8	10.3	5.7	7.7	0.5926

[a] the weights and the weighted differences are also listed for comparison with table 3b. GOF = 13.6; R = 0.031.
[b] GOF = 4.6; R = 0.36.

tion is not straightforward, even neglecting the uncertainties in the data. The strong mass transport on the Ge(111) surface as revealed by the facetting due to Ag atoms [8] may cause incomplete substrate layers. This would change the reference to which occupation is scaled. Due to the large uncertainties the high Debye–Waller factors of both Ag ($B_{Ag} = 6.9 \pm 0.6$) and Ge ($B_{Ge} = 2.9 \pm 0.4$) should not be overinterpreted.

Because only fractional-order in-plane diffraction data were measured, no conclusions can be made about the structure in the direction normal to the surface, nor about the registry of the reconstructed atoms to the bulk lattice. However, theoretical calculations predict the 3-fold coordinated hollow site below the substrate surface to be energetically preferred adsorption site for both adsorbates, Au and Ag, on Ge(111) and Si(111) [15]. This absorption site seems to be plausible for the further reason that the observed substrate

distortions would then occur in the top-most substrate layer. The cohesive forces between the Ag atoms result in the formation of trimer clusters and may be responsible for the slight shift of the Ag atoms away from the ideal, highly symmetric H3 site. The substrate atoms are shifted towards the unoccupied H3 sites, forming trimers as well. Fig. 2b shows the projection of one split-domain.

Further calculations have been made for models similar to that found for Ag/Si(111) [11,12]. In that structure the trimers are formed by Si atoms and the Ag–Ag distance is 3.45 Å, clearly longer than the Ag bulk value. This model is obviously different from the trimer model discussed above. The optimum R value obtained in a structure refinement choosing the HCT-1 (honeycomb chained trimer) or HCT-2 models of ref. [11], which are identical in projection, were $R = 0.072$ using unit weights and $R = 0.62$ using individual weights. Both R values are clearly
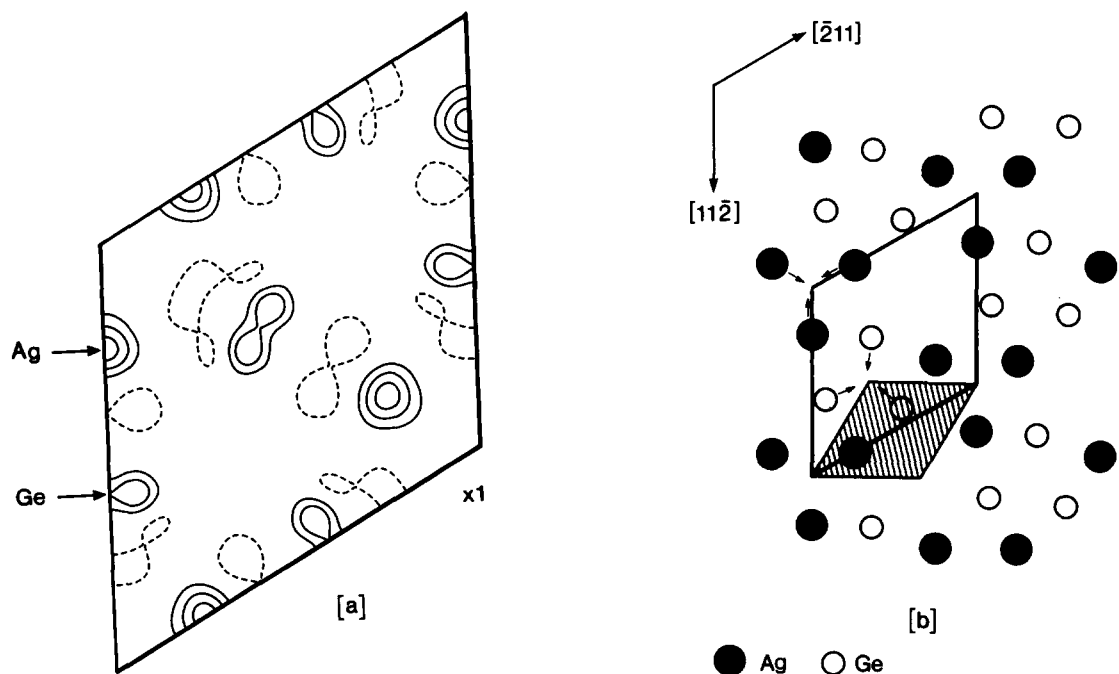

Fig. 2. (a) Electron-density map of final model refined with unit weights. (b) Model for the $\sqrt{3} \times \sqrt{3}$ superstructure. The hatched area marks a 1 × 1 substrate cell.

worse than the optimum values for the trimer model. We therefore can rule out the HCT models.

4. Conclusions

We have shown that Ag on Ge(111) forms trimer clusters and behaves very similar to the recently characterized system Au on Si(111) [9]. The interatomic distance within the trimer clusters is close to the Ag bulk value. The structure is different from the Ag/Si(111) surface. In this system the Ag atoms do not form trimer clusters and the reconstructed substrate atoms are not shifted normal to the mirror plane [11]. The atoms of at least one substrate layer seem to be shifted towards bridge positions between Ag atoms of neigboring trimers. Finally the trimer layer which could have an ideal coverage of $\theta_{Ag} = 1$ ML is underoccupied as is the case for Au/Si(111).

Acknowledgements

References

[1] G. Le Lay, Surf. Sci. 132 (1983) 169.

[2] B.J. Knapp, J.C. Hansen, M.K. Wagner, W.D. Clendening and J.G. Tobin, Phys. Rev. B 40 (1989) 2814.

[3] B.J. Knapp and J.G. Tobin, Phys. Rev. B 37 (1988) 8656.

[4] G. Le Lay, J. Vac. Sci. Technol. B 1 (1983) 354.

[5] W.C. Fan and A. Ignatiev, Phys. Rev. B 40 (1989) 5479.

[6] M. Bertucci, G. Le Lay, M. Manneville and R. Kern, Surf. Sci. 85 (1979) 471.

[7] M. Chester and T. Gustafsson, Phys. Rev. B 42 (1990) 9233.

[8] E. Suliga and M. Henzler, J. Vac. Sci. Technol. A 1 (1983) 1507.

[9] D. Dornisch, W. Moritz, H. Schulz, R. Feidenhans'l, M. Nielsen, F. Grey and R.L. Johnson, Phys. Rev. B 44 (1991) 11221.

[10] M.J. Buerger, Vector Space and its Application in Crystal Structure Investigation (Wiley, New York, 1959).

[11] E. Vlieg, E. Fontes and J.R. Patel, Phys. Rev. B 43 (1991) 7185, and references therein.

[12] Y.G. Ding, C.T. Chan and K.M. Ho, Phys. Rev. Lett. 67 (1991) 1454.

[13] See, for example: M.M. Woolfson, An Introduction to X-ray Crystallography (Cambridge University Press, London, 1970).

[14] $R = [\Sigma(w(F_o^2 - F_c^2)^2)/\Sigma(wF_o^4)]^{1/2}$; $w = 1/\sigma^2(F_o^2)$; $GOF = \chi^2/(N - p)$, with $\chi^2 = \Sigma[(F_o^2 - F_c^2)^2/\sigma^2(F_o)]$ and $\sigma(GOF) = 1/(N - p)^{1/2}$; N is the number of observables, p the number of parameters.

[15] J. Che, K. Zhang and X. Xie, Proc. 17th Int. Conf. Phys. Semicond., 1984, Eds. J.D. Chadi and W.A. Harrison (Springer, New York, 1985) p. 121.